

CHAPTER II
ANA AND GIS ZEOLITES SYNTHESIS DIRECTLY FROM
ALUMATRANE AND SILATRANE BY SOL-GEL PROCESS AND
MICROWAVE TECHNIQUE

(Journal of European Ceramic Society, 22 (2000) 2305-2314)

2.1 Abstract

Alumatrane and silatrane were successfully used as precursors to produce aluminosilicate via the sol-gel process. Due to their ability in retarding hydrolysis process, forming meso-porous material was easier. Both NaCl and NaOH can be used as hydrolysis agent, however, NaOH had highly influenced in crystalline formation. The higher NaOH concentration, the better crystalline formation was observed. Gel transformation was an endothermic reaction. The maximum transformation occurred at 106°C, as determined by DSC. By using NaOH/H₂O as a hydrolysis agent and treating amorphous metal oxide gel by microwave technique, the crystalline aluminosilicate was formed and narrow particle size distribution was obtained. By fixing the ratio of SiO₂, Al₂O₃, Na₂O and H₂O at 1:0.25:3:410, GIS was synthesized at hydrothermal treatment of 3 h at 110°C, while ANA was produced at 130°C for 8 h. GIS obtained had 4.55 μm in size while ANA's size was 9.96 μm.

Keywords: Alumatrane, Silatrane, Microwave technique, Sol-gel process, and Zeolite

2.2 Introduction

Zeolites or crystalline aluminosilicates are widely used in separation and refinery industries as catalysts, adsorbents and ion exchangers due to their meso and micro-porous structures¹. Most of zeolites used come from either nature or synthesis. Synthetic zeolites are obtained via the sol-gel process to firstly produce amorphous gel from an interaction between aluminate and silicate or silica sol. To obtain any crystalline phase, further hydrothermal treatment is needed. This treatment can be conducted by either conventional or microwave heating. Microwave heating is a fast and energy efficient technique, which prevents other side reactions owing to their exact nature in interaction². Energy transfer from microwave to material occurs either through resonance or relaxation, resulting in rapid heating, causing simultaneous, abundant nucleation and fast dissolution of gel²⁻⁵. These advantages enhance the crystallization rate in very short time, leading to small particle size with narrow particle size distribution and high purity⁵.

Generally, the starting materials used for zeolites synthesis are metal salts (metal aluminate and metal silicate or silica sol) or metal alkoxides. In some cases, such as high silica zeolites or hexagonal structure type, the association of organic templates is necessary. Organic parts incorporate with inorganic parts via the so-called self-assembling process to form inorganic-organic micelle. The process organizes metal ions to form particle nuclei, flocculating after a more or less lengthy growing state⁶⁻⁹. Organic templates generally and successfully used are crownethers or tertiary ammonium salts. However, surfactants at around the critical (CMC) point are also employed in some works. This technique leads to gels and meso-structure materials but does not go forward to meso-porous solid due to the obstruction of the remaining organic portions. Moreover, micelle formation also increases flocculating stability, reducing film drainage and coalescence¹⁰⁻¹¹. Metal alkoxides are sometimes used to increase the self-assembling ability since their organic parts can incorporate in micelle and their hydrolytic inertness increases as increasing both the size of the organic parts (steric effect) and the number of alcohol groups in the ligand (chelate or cage effect).

Analcium (ANA) and Na-P1 (GIS) are of importance and interest, especially, ANA, which has ability in matrix storage for radioactive materials¹². ANA is produced at 130° - 160°C using Teflon-lined autoclave (conventional heating) and aluminum sulfate/sodium metasilicate as precursors, at 165° -185°C using CTAB as a template at pH 10 – 12.5 or at 1300°C if started from nanostructured KAlSiO₄ precursor¹³⁻¹⁶. GIS can be synthesized from natural clay, such as Kaolinite, Aidoudi, by crystallization at 75° – 85°C. The reaction time varies depending on clay types, which can be 1 to 60 days¹⁷⁻¹⁸. GIS can also be synthesized either from fly ash waste from power plants by fusion followed by crystallization at 90°C for 7 days¹⁹ or from nuclear waste solution by crystallization at 45°-90°C²⁰. However, GIS obtained from the mentioned methods are mostly used as molecular sieve owing to its low purity.

Hence in this work, both synthesized silatranes and alumatranes were chosen as precursors for zeolite synthesis due to their ability in constructing inorganic-organic micelle. Other organic templates and surfactants have thus no need in the system. Moreover, these atranes are thermodynamically stable in an aqueous-base system since they can form complexes with metal ion to increase the possibility of expanding its coordinated sphere. This phenomenon will moderate the alkoxides reactivity towards the nucleophilic attack of water, as a result, it retards the precipitation to occur^{11,21-22}. These properties remarkably induce the ability in forming meso-porous framework materials.

2.3 Experimental

2.3.1 Materials

Fumed silica (SiO₂, surface area 473.5 m²/g, average particle size of 0.007 μm) and aluminum hydroxide hydrate (Al(OH)₃, surface area 50.77 m²/g), were purchased from Sigma Chemical Co. and used as received. Triethanolamine (TEA, N(CH₂CH₂OH)₃), and triisopropanolamine (TIS, N(CH₂CHCH₃OH)₃) were supplied by Carlo Erba Reagenti and Fluka Chemical AG., respectively. Both were used as received. Ethylene glycol (EG, HOCH₂CH₂OH) was obtained from J.T.

Baker Inc. and distilled using fractional distillation prior to use. Sodium hydroxide (NaOH) and sodium chloride (NaCl) were purchased from EKA Chemicals and AJAX Chemicals, respectively. Both were used as received. Acetonitrile (CH₃CN) was obtained from Lab-Scan Co., Ltd. and distilled using standard purification method.

2.3.2 Instrumentals

FTIR spectroscopic analysis was conducted using Bruker Instrument (EQUINOX55) with a resolution of 4 cm⁻¹. The solid samples were prepared by mixing 1% of sample with dried KBr, while the liquid samples were analyzed using Zn-Se window cell. Mass spectra were obtained using a VG Autospec model 7070E from Fison Instrument with VG data system, using the positive fast atomic bombardment (FAB⁺-MS) mode and glycerol as a matrix. CsI was used as a reference, while a cesium gun was used as an initiator. The mass range used was from $m/e = 20$ to 3,000. Thermal properties were analyzed using thermogravimetric analysis (TGA) and differential scanning calorimetry (DSC) mode. TGA was performed with sample size of 10 – 20 mg using Perkin Elmer instrument: TGA7 analyzer while DSC was conducted with sample size of 5 – 10 mg on Netzsch instrument: DSC200 Cell at a heating rate of 10°C/min under nitrogen atmosphere. For liquid and gel samples, high-pressure gold cell was used with the sample size of 10-20 mg. Crystallinity of products were characterized using Rigaku X-Ray Diffractometer at scanning speed of 5 degree/sec, CuK α as a source and CuK β as a filter. The working ranges were 5 – 90 and 5 – 50 theta/2 theta. SEM micrographs were performed using a JEOL 5200-2AE scanning electron microscope. Electron Probe Microanalysis (EPMA) was used to analyze sample in micro-scale for both qualitative and quantitative analysis of element, using X-Ray mode detector (SEM/EDS). Particle size was determined using Mastersize X Ver.2.15, Malvern Instruments. Water was used as a mobile phase. Hydrothermal treatment by microwave heating technique was conducted using MSP1000, CME Corporation (Spec. 1,000W and 2,450 MHz). Samples were heated in Teflon-lined digestion vessel using inorganic digestion mode with time-to-temperature program.

2.3.3 Precursors Synthesis

2.3.3.1 Silatrane Synthesis (Si-TEA)

Wongkasemjit's synthetic method²³ was used by mixing silicon dioxide, 0.10 mol, and triethanolamine, 0.125 mol, in a simple distillation set using 100 mL ethylene glycol, as solvent. The reaction was done at the boiling point of ethylene glycol under nitrogen atmosphere to remove water as a by-product and ethylene glycol from the system. The reaction was set for 10 h and the rest of ethylene glycol was removed under vacuum (10^{-2} torr) at 110°C. The brownish white solid was washed with dried acetonitrile for three times. The white powder product was characterized using FTIR, TGA, DSC and FAB⁺-MS.

FTIR: 3000-3700 cm^{-1} (w, intermolecular hydrogen bonding) 2860-2986 cm^{-1} (s, $\nu\text{C-H}$), 1244-1275 cm^{-1} (m, $\nu\text{C-N}$), 1170-1117 (bs, $\nu\text{Si-O}$), 1093 (s, $\nu\text{Si-O-C}$), 1073 (s, $\nu\text{C-O}$), 1049 (s, $\nu\text{Si-O}$), 1021 (s, $\nu\text{C-O}$), 785 and 729 (s, $\delta\text{Si-O-C}$) and 579 cm^{-1} (w, $\text{Si} \leftarrow \text{N}$). TGA: one mass loss transition at 390°C and 18.47 %ceramic yield corresponding to $\text{Si}((\text{OCH}_2\text{CH}_2)_3\text{N})_2\text{H}_2$. DSC: 349°C (endothermic) and 373°C (exothermic). FAB⁺-MS: approximately 3% of the highest m/e at 669 of $\text{Si}_3((\text{OCH}_2\text{CH}_2)_3\text{N})_4\text{H}^+$ and 100% intensity at 323 of $\text{Si}((\text{OCH}_2\text{CH}_2)_3\text{N})_2\text{H}_3^+$.

2.3.3.2 Alumatrane Synthesis (Al-TIS)

The synthetic method followed Wongkasemjit's work²⁴ by mixing aluminum hydroxide, 0.10 mol, and triisopropanolamine, 0.125 mol, in a simple distillation set, using ethylene glycol as solvent. The reaction mixture was heated to the boiling point of ethylene glycol under nitrogen atmosphere for 10 h to remove water as a by-product and ethylene glycol from the system. The rest of ethylene glycol was removed by heating at 110°C under vacuum (10^{-2} torr). The crude product was washed with dried acetonitrile for three times and characterized using FTIR, TGA, DSC and FAB⁺-MS.

FTIR: 3000-3700 cm^{-1} (s, intermolecular hydrogen bonding) 2860-2986 cm^{-1} (m, $\nu\text{C-H}$), 1649 (w, O-H overtone), 1244-1275 cm^{-1} (w, $\nu\text{C-N}$), 1130 (m, $\nu\text{C-O}$), 1102 (s, $\nu\text{Al-O-C}$), 1037 (m, $\nu\text{C-O}$), and 649 (s, $\delta\text{Al-O}$). TGA: two mass loss transitions at 139° and 393°C and 23.97 %ceramic yield corresponding to $\text{Al}(\text{OCHCH}_3\text{CH}_2)\text{N}$. DSC: 196°C (endothermic) and 380°C (exothermic). FAB⁺-

MS: approximately 4% of the highest m/e at 1292 of $(\text{Al}(\text{OCHCH}_3\text{CH}_2)\text{N})_6\text{H}^+$ and 100% intensity at 216 of $\text{Al}(\text{OCHCH}_3\text{CH}_2)\text{NH}^+$.

2.3.4 Sol-Gel Process and Microwave Technique

SiTEA and ALTIS were mixed with NaOH or NaCl solution at room temperature at a ratio of $\text{SiO}_2:0.25\text{Al}_2\text{O}_3:x\text{Na}_2\text{O}:y\text{H}_2\text{O}$ (where $0 \leq x \leq 10$ and $63 \leq y \leq 1000$). The solution mixture was aged overnight and then transferred to Teflon vessel for further hydrothermal treatment using microwave technique. The solution mixtures containing various ratio of $\text{SiO}_2:0.25\text{Al}_2\text{O}_3:x\text{Na}_2\text{O}:y\text{H}_2\text{O}$ were hydrothermally treated for various time and the resulting white powder products were washed three time using distilled water. The products were finally dried overnight at 75°C. According to the results of this work the gel started to form at $\text{SiO}_2:\text{Na}_2\text{O}$ ratio of 1:0.0069 and the best ratio of $\text{SiO}_2:\text{Na}_2\text{O}$ for synthesizing ANA and GIS was ranged from 1:2 to 1:3. To obtain homogeneous dispersion of powder product in the solution mixture, water needed to be started at $y = 63$, and the suitable $\text{SiO}_2:\text{H}_2\text{O}$ ratio for synthesizing ANA and GIS was 1:410.

2.3.5 Characterization

The functional groups of the precursor and transformed gel were measured by FTIR while the thermal stability and properties were obtained from TGA and DSC. The crystallinity of aluminosilicate products was characterized using XRD. The morphology of the aluminosilicate products was observed using SEM whereas the compositions of these products were tested by EDS-SEM, using X-Ray mode detector. The particle size and particle size distribution of synthesized products were measured using particle size analyzer containing water as a mobile phase.

2.4 Results and Discussion

2.4.1 Precursor Synthesis

Silatrane and alumatrane were successfully synthesized by Oxide-One-Pot-Synthesis (OOPS) process directly from silica and alumina. The reactions are the condensation reaction, generating water as a by-product. Thus, removal of water from the system drives the reactions forward. The products were crystallized out when most of ethylene glycol were removed under vacuum and purified by washing with dried acetonitrile to remove the other organic residuals. The products can absorb moisture and then undergo hydrolysis process, thus need to be kept under vacuum.

2.4.2 Sol-Gel Process

Cabrera¹¹ synthesized aluminosilicate having uniform pore from silatrane and alumatrane in CTAB/TEA/H₂O system via the sol-gel process. The major drawback of his work is that he was unable to obtain aluminosilicate with framework structure. The reason comes from the organic content in the system obstructing the framework formation. In this work, either NaOH or NaCl/H₂O solution was thus chosen to be used in the sol-gel process to avoid the extra organic content in the system. The framework structure of aluminosilicate has occurred by joining tetracoordinated (SiO₄)⁴⁻ with tetracoordinated (AlO₄)⁵⁻ causing myriad of lattice architectures which consisted of channels and cages with different types of connectivity²⁵. Negative charges on Al-atoms in the framework are stabilized by the Na cation in the system.

FTIR was employed to follow the hydrolytic reaction of both silatrane and alumatrane in NaOH or NaCl/H₂O solution, as shown in Figure 1. As can be seen in the NaOH system, the Si-O-C and Al-O-C regions, 1000-1170 cm⁻¹ were changed significantly. The peak at 1049 cm⁻¹ referring to Si-O-Si was higher and broader, while the peak at 1102 cm⁻¹ corresponding to Al-O-Al was slightly shifted to higher frequency and became broader. The C-O-M (M = Si or Al) peak at 1021 cm⁻¹ was also reduced due to the organic ligand, TEA, cleaved from the system. This was confirmed by the reduction of C-N peak at 1275 cm⁻¹. By curve

fitting the area under the peak at 1275 cm^{-1} (C-N peak, representing organic ligand concentration), the approximate rate of hydrolysis during the sol-gel process was determined and is shown in Figure 2. The rate of hydrolysis was faster with hydroxyl anion (OH^-). The hydroxyl ion attacked Si- or Al-atom faster and easier to form hydroxide in the hydrolysis step. The hydroxyl group of metal hydroxide part reacted with Si- or Al-atom of other group to form metal-oxygen-metal bridge and release organic part in the condensation step. With both anions, the rate of hydrolysis shows two distinct regimes; during the first hour the rate of hydrolysis is rapid followed by a much slower rate.

In case of $\text{NaCl}/\text{H}_2\text{O}$ system, chloride ion attacked Si- or Al-atom in the same manner. However, the attack rate of chloride ion is assumed to be slower due to the lower electronegativity of M-Cl bond and larger ionic radii of Cl^- ²⁶. Hence, the hydrolysis rate of NaCl/water system was slower than that of $\text{NaOH}/\text{H}_2\text{O}$ system.

2.4.3 Transformation to Aluminosilicate

After the gel was formed, the gel transformation to aluminosilicate by hydrothermal treatment was first studied using DSC high-pressure cell (Figure 3) to investigate where the maximum transformation should be. It was found that the transformation was certainly endothermic reaction, in agreement with Yang work²⁷ due to the dissolution of amorphous metal-oxide network and crystallization of aluminosilicate²⁸⁻²⁹. The transition started at 103°C and the maximum transformation occurred at 106°C . The overall energy consumption was 35.93 J/g . After the second run, there was no peak shown up, indicating that the gel had already transformed into a crystalline aluminosilicate.

Transformation of the gel into crystalline products depended on many factors, and sodium hydroxide concentration was one of them. The higher the sodium hydroxide concentration used, the higher crystallinity was obtained. This is due to the negative charges contained in the framework structure. These charges need to be stabilized by sodium cations³⁰. As we found from the XRD shown in Figure 4, once the sodium hydroxide concentration was high enough, increasing

sodium hydroxide concentration would not have further effect. Although the loading of Si:Al ratio was changed from 2:1 to 87:1, the same product was obtained, as illustrated in Figure 5. Comparing with the literature data result, this product was exactly ANA zeolites consisting of distorted T6-ring chains, which have distorted 4-rings in between, as can be seen in Figure 6. The crystal data are listed in table 1.

Another factor affecting the final product structure was microwave-heating temperatures. As shown in Figure 7, lowering the heating temperature resulted in different phase formation. Below 110°C, only amorphous was observed. At 110°C, GIS structure type was observed. Secondary building unit (SBU) was formed from T16 units, two 8-rings connected as a crankshaft chain. Periodic building unit (PBU) was formed when two crankshaft chains and T4-rings were connected in such a way that the cylinder with a T8-ring pore was formed. Each PBU's was connected through T4-rings see Figure 8. By comparing these two structures, it might be said that higher energy given made the framework be distorted and arranged itself in a more perfect tetrahedral form.

2.4.4 Effect of Crystallization Conditions

Crystallization conditions of both products, ANA and GIS, were studied at two different temperatures, 110°C and 130°C and at the Si:Al:Na ratio of 2:1:6 as a function of microwave heating time. At 130°C, both phases were obtained at different times (Figure 9). GIS was completely built first at 80 min. After 240 min, ANA was observed and the pure phase was formed after 480 min (or 8 h) of thermal treatment. The atomic ratio of Si:Al:Na was also varied with time. At the Si:Al ratio loading at 2:1, the amorphous product obtained was at 1.86:1 which was closer to the loading ratio. After GIS was formed, the ratio dropped to ~1.71:1 which was closely matched with XRD PDF#39-0219 having $\text{Na}_6\text{Al}_6\text{Si}_{10}\text{O}_{32}\cdot 12\text{H}_2\text{O}$ ~ Si:Al:Na= 1.67:1:1. It is not a perfect matching due to the presence of very small fraction of ANA formed after 100 min (Figures 10-11). Although amount of ANA was higher as the time went longer, the Si:Al ratio was still the same until it reached 300 min. The Si:Al ratio was increased to 2:1 at 480 min that was the same as XRD PDF#19-1180 containing $\text{Na}(\text{Si}_2\text{Al})\text{O}_6\cdot\text{H}_2\text{O}$ ~ Si:Al:Na = 2:1:1. SEM coincidentally

indicated the same phenomena as XRD. GIS product was formed in a cubic shape, and particle sizes increased as increasing time. However, very small round particles of ANA-C were observed after 100 min in cubic form while at 200 min ANA-O was clearly observed in an octagonal form. The particle size was also bigger and number of particle size was increased with time while GIS particle size was reduced. The fully population of ANA particles was produced at 480 min.

At heating temperature of 110°C, only GIS product was observed in both XRD (Figure 12) and SEM (Figure 13). The Si:Al ratio was reduced from ~1.90:1 to ~1.65:1. All these results indicated that the fully GIS was produced at 180 min and only GIS was obtained even it was heated for 15 h.

By comparing these two heating temperatures, pure GIS could be made at 110°C for 180 min, while at 130°C, the purity of GIS is decreased due to the formation of ANA. The higher energy initiated ANA nuclei made from 6,4 SBSs which is more stable than 8,4 SBUs of GIS. Moreover, by heating at 110°C, GIS had only one particle size distribution which falls in-between 1.32 to 14.08 μm with the mean diameter of 4.55 μm , while at 130°C ANA product had 3 particle size distributions. 11.42% of ANA particles had less than 3 μm . The major product size was in range of 3 – 37.79 μm (88.04%). The mean average particle size was 6.02 μm while the maximum population was at 9.96 μm . Based on SEM, the smallest group might be ANA-C while the biggest population was ANA-O. The highest particle sizes came from the agglomeration of the particle. As compared with data obtained from SEM magnified at x5,000, the average particle size of GIS was 3.67 μm and ANA 8.85 μm . They were slightly lower than those obtained from particle size analyzer.

2.5 Conclusions

Silatrane and alumatrane can undergo the sol-gel process followed by hydrothermal treatment in the presence of NaOH to provide GIS and ANA zeolites with uniform particle size and narrow particle size distribution, as observed by SEM and particle size analyzer. Appropriate NaOH concentration is added to allow the

crystalline aluminosilicate to be formed due to the role of stabilization. By fixing the ratio of $\text{SiO}_2:\text{Na}_2\text{O}$ at 1:3, heating temperature at 130°C , and varying the Si:Al ratio of 2:1 to 87:1, only ANA products are obtained. Lowering the microwave heating temperature provides the phase transformation from ANA to GIS, which has less packing structure (framework density = $15.3 \text{ T}/1000\text{\AA}^3$ for GIS while $18.5 \text{ T}/1000\text{\AA}^3$ for ANA). At the ratio of $\text{SiO}_2:0.25\text{Al}_2\text{O}_3:3\text{Na}_2\text{O}: 410\text{H}_2\text{O}$, GIS can be completely formed in 180 min at heating temperature of 110°C with the particle size of $4.55 \mu\text{m}$ while ANA is perfectly found in 480 min at heating temperature of 130°C with the particle size of $9.96 \mu\text{m}$.

2.6 Acknowledgement

This research work was fully supported by the Thailand Research Fund (TRF).

2.7 References

1. H. VanBekum, E. M. Flanigen, J. C. Jensen (Eds), "The preparation of molecular sieves. A. Synthesis", *Introduction to Zeolite Science and Practice*, Elsevier, Amsterdam, 1991
2. K. J. Rao, B. Vaidhyanathan, M. Ganguh, P. A. Ramakrishnan, "Synthesis of Inorganic Solid Using Microwave", *Chem. Mater.*, 1999, 11, 882
3. J. C. Jansen, A. Arafat, A. K. Barakat, H. VanBekum, "Microwave Technique in Zeolite Synthesis", *Synthesis of Micro Porous Materials*, Vol.1, Van Nostrand Reinhold, New York, 1992
4. C. S. Cundy, "Microwave Techniques in the Synthesis and Modification of Zeolite Catalyst A. Review", *Collect. Czech. Chem. Commun.*, 1998, 63, 1699
5. X. Xu, W. Yang, J. Liu, L. Lin, "Synthesis of a High-Pressure NaA Zeolite Membrane by Microwave Heating", *Adv. Mater.*, 2000, 12, No.3, 1995

6. C. Kresge, M. Leonowicz, M. Roth, J. Vartuli, J. Beck, "Ordered Mesoporous Molecular Sieves Synthesized by a Liquid-Crystal Template Mechanism", *Nature*, 1992, 359, 710
7. A. Corma, "From Microporous to Mesoporous Molecular sieve Materials and their Use in Catalyst", *Chem. Rev.*, 1997, 97, 2373
8. J. Ying, C. Mehnert, M. Wong, "Synthesis and Applications of Supramolecular Templated Mesoporous Materials", *Angew. Chem. Int. Ed. Engl.*, 1999, 38, 56
9. A. Monnier, F. Schuth, Q. Huo, D. Kumar, D. Margolese, R. Maxwell, G. Stucky, M. Krishnamurty, P. Petroff, A. Firouzi, J. Janiche, B. Chmelka, "Cooperative Formation of Inorganic-organic Interfaces in the Synthesis of Silicate Mesostructure", *Science*, 1993, 261, 1290
10. D. Antonelli, J. Ying, "Synthesis of Hexagonally Packed Mesoporous TiO₂ by a modified Sol-gel Method", *Angew. Chem. Int. Ed. Engl.*, 1995, 34, 2014
11. S. Cabrera, J. E. Haskouri, C. Guillem, J. Latorre, A. Beltran-Porter, D. Beltran-Porter, M. D. Marcos, P. Amoros, "Generalised Synthesis of Ordered Mesoporous Oxides, the Altrane route", *Solid State Science*, 2000, 2, 405
12. J. L. Anchell, J. C. White, M. R. Thompson, A. C. Hess, "An AB-initio Periodic Hartree-Fock Study of Group IA Cations in ANA-Type Zeolite", *J. of Phy. Chem.*, 1994, 98, 4463
13. G. S. Wiersema, R. W. Thompson, "Nucleation and Crystal Growth of Analcime from Clear Aluminosilicate Solution", *J. Mater. Chem.*, 1996, 6/10, 1693
14. Y. Yokomori, S. Idaka, "The Crystal Structure of Analcime", *Micropor. Mesopor. Mat.*, 1998, 21/4-6, 365
15. L. M. Huang, X. Y. Chen, Q. Z. Li, "Synthesis of Microporous Molecular Sieve by Surfactant Decomposition", *J. Mater. Chem.*, 2001, 11/2, 610
16. R. Dimitrijevic, V. Dondur, "Synthesis and Characterization of KAlSiO₄ Polymorphs on the SiO₂-KAlO₂ Join 2 The End-member of ANA Type of Zeolite Framework", *J. of Solid State Chem.*, 1995, 115, 214
17. L. V. C. Rees, S. Chandrasekhar, "Hydrothermal Reaction of Kaolinite in Presence of Fluoride Ions at Ph-Less-Than-10", *Zeolites*, 1993, 13, 535

18. A. Baccouch, E. Srasra, M. El Maaoui, "Preparation of Na-P1 and sodalite octahydrate zeolites from Interstratified Illitesmectite", *App. Clay Sci.*, 1998, 13, 255
19. A. Srinivasan, M. W. Grutzeck, "The adsorption of SO₂ by Zeolites Synthesized from Fly Ash", *Env. Sci & Tech.*, 1999, 33, 1464
20. A. Katz, A. R. Brough, R. J. Kirkpatrick, L. J. Struble, J. F. Young, "Effect of Solution Concentration on the Properties of a Cementitious Grout Wasteform for Low-level Nuclear Waste", *Nuclear Tech.*, 2000, 129, 236
21. P. E. A. DeMoor, T. P. M. Bcelen, R. A. VanSanten, L. W. Beck, M. E. Davis, "Si-MFI Crystallization Using a "Dimer" and "Trimer" of TPA Studied with Small-Angle X-Ray Scattering", *J. Phys. Chem. B*, 2000, 104, 7600
22. C. Frye, G. Vicent, W. Finzel, "Pentacoordinate Silicon Compounds V^{1a}. Novel Silatrane Chemistry", *J. Am. Chem. Soc.*, 1971, 93, 6805
23. P. Piboonchaisit, S. Wongkasemjit and R. Laine, "A Novel Route to Tris (silatranxyloxy-*I*-propyl)amine Directly from Silica and Triisopropanolamine, Part I", *Science-Asia, J. Sci. Soc. Thailand*, 1999, 25, 113
24. Y. Opornsawad, B. Ksapabutr, S. Wongkasemjit, R. Laine, "Formation and Structure of Tris(alumatranxyloxy-*I*-propyl)amine Directly from Alumina and Triisopropanolamine", *Eur. Polym. J.*, 2001, 37/9, 1877.
25. A. Dyer, "The structure of Zeolites" *An Introduction to Zeolite molecular sieves*, John Wiley and Sons, New York, 1988
26. E. M. Rabinovich, "Particulate silica gels and glasses from the sol-gel process", *Sol-Gel Technology For Thin Films, Fibers, Performs, Electronics and Specially Shapes*, Noyes Publication, New Jersey, 1988
27. S. Yang, A. Navrotsky, B. L. Phillips, "In Situ Calorimetric, Structural, and Composition Study of Zeolite Synthesis in the System 5.15Na₂O-1.00Al₂O₃-3.28SiO₂-165H₂O", *J. Phys. Chem. B.*, 2000, 140, 6071
28. R. M. Barrer, *The Hydrothermal Synthesis of Zeolites*, Academic Press, London, 1983
29. R. Szostak, "Fundamental of Synthesis", *Molecular Sieves-Principles of Synthesis and Identification*, Van Nostrand Rheinhold, New York, 1989

30. C. Brinker, G. Scherer, "The Physics and Chemistry of Sol-Gel Processing", *Sol-Gel Science*, Academic, New York, 1990

Table 2.1 Results of Crystal Analysis

Name	Analcime	Na-P1
Type	ANA	GIS
Crystal System	cubic for ANA-C octagonal for ANA-O	tetragonal
Space Group (SG)	Ia-3d	I-4 3d
a (Å)	13.74	9.997
b (Å)	13.74	9.997
c (Å)	13.74	9.997
Unit cell volume (Å ³)	2593.94	999.04
λ (Cu-K α) (Å)	1.54056	1.54056
Filter	Cu-K β	Cu-K β
Data collection range (2 θ , deg.)	5-50	5-50
Data collection instrument	Rigoku X-ray Diffractometer	Rigoku X-ray Diffractometer
Matched PDF#	41-1478 for ANA-C 19-1180 for ANA-O	39-219

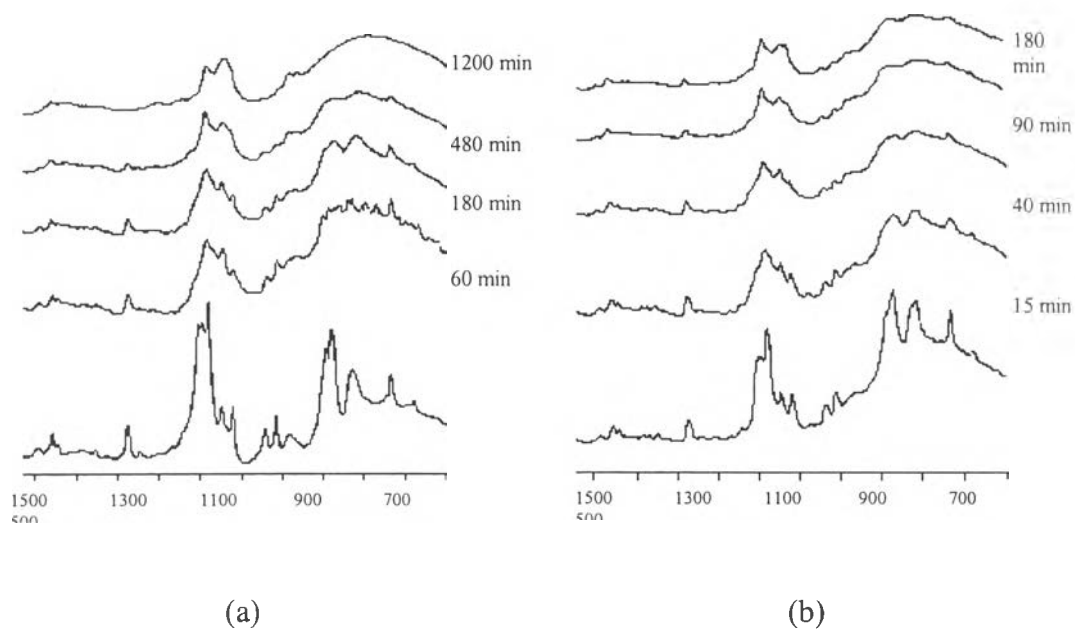
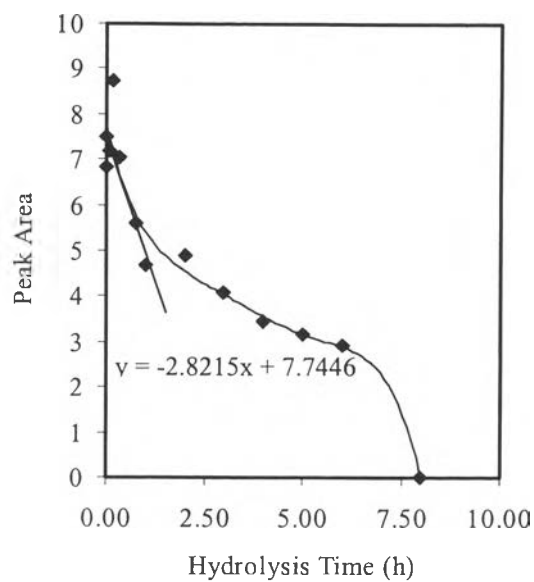
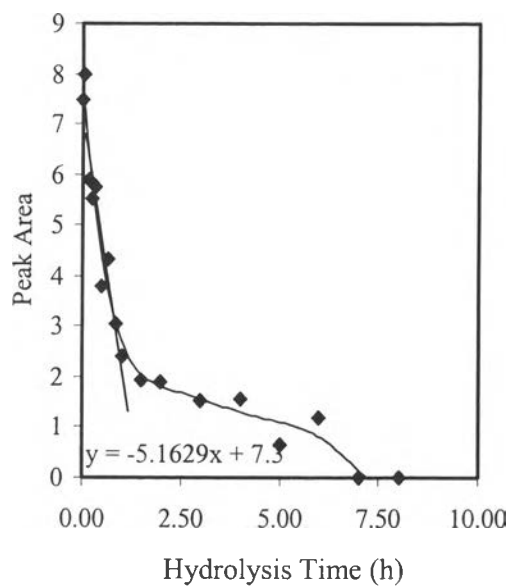


Figure 2.1 Hydrolysis behavior of aluminosilicate mixture at the ratio of 1SiO₂:0.5Al₂O₃:0.096Na₂O: 63H₂O in (a) NaCl/H₂O System and (b) NaOH/H₂O System



(a)



(b)

Figure 2.2 Reduction rate of vC-N peak at 1275 cm⁻¹ of the mixture containing 1SiO₂:0.5Al₂O₃:0.096Na₂O: 63H₂O in (a) NaCl/H₂O and (b) NaOH/H₂O systems

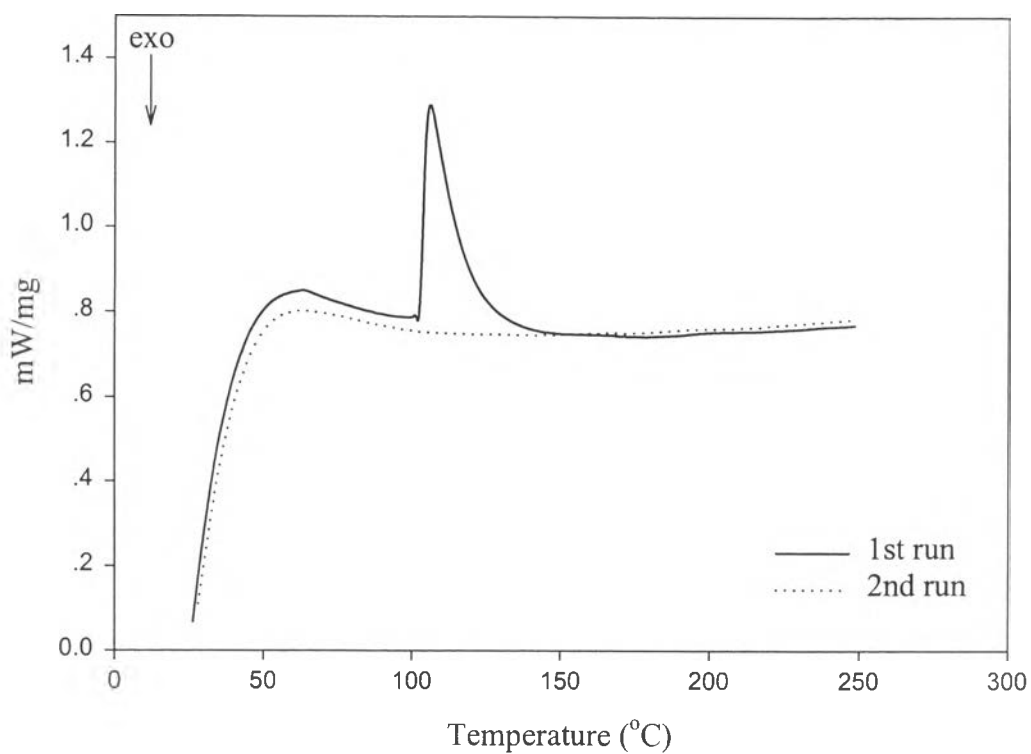


Figure 2.3 Thermal property of gel transformation to aluminosilicate using high pressure DSC cell at heating rate of 10°C/min and 1SiO₂:0.5Al₂O₃: 0.7Na₂O: 410H₂O

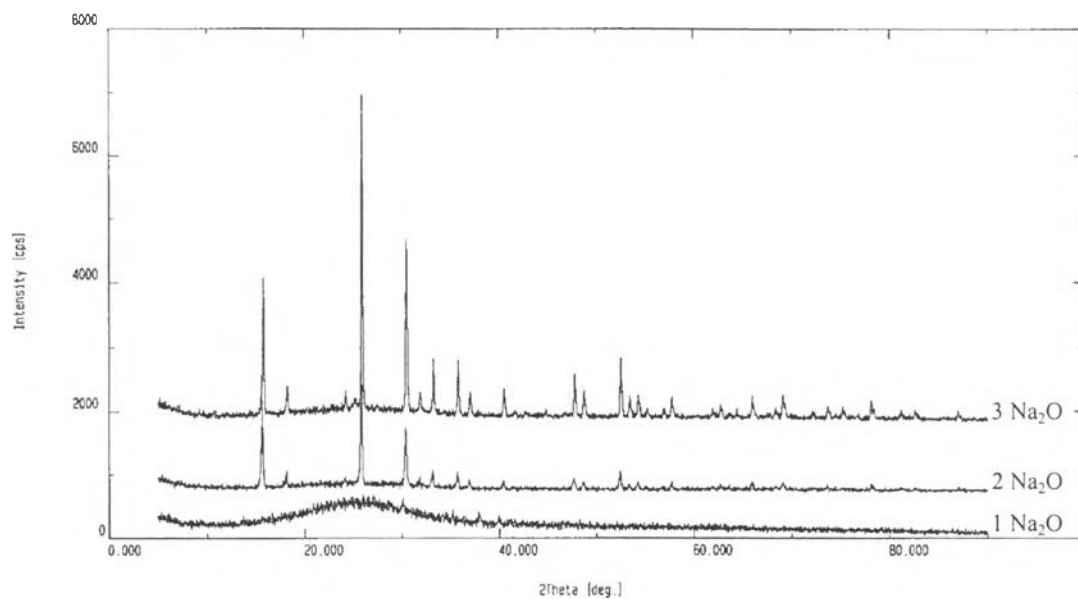


Figure 2.4 Effect of NaOH concentration on microwave heated aluminosilicate synthesized from $1\text{SiO}_2:0.0115\text{Al}_2\text{O}_3:x\text{Na}_2\text{O}:410\text{H}_2\text{O}$ ($\text{Si}:\text{Al} = 87:1$, $x = 1 - 3$) at $150^\circ\text{C}/15\text{h}$

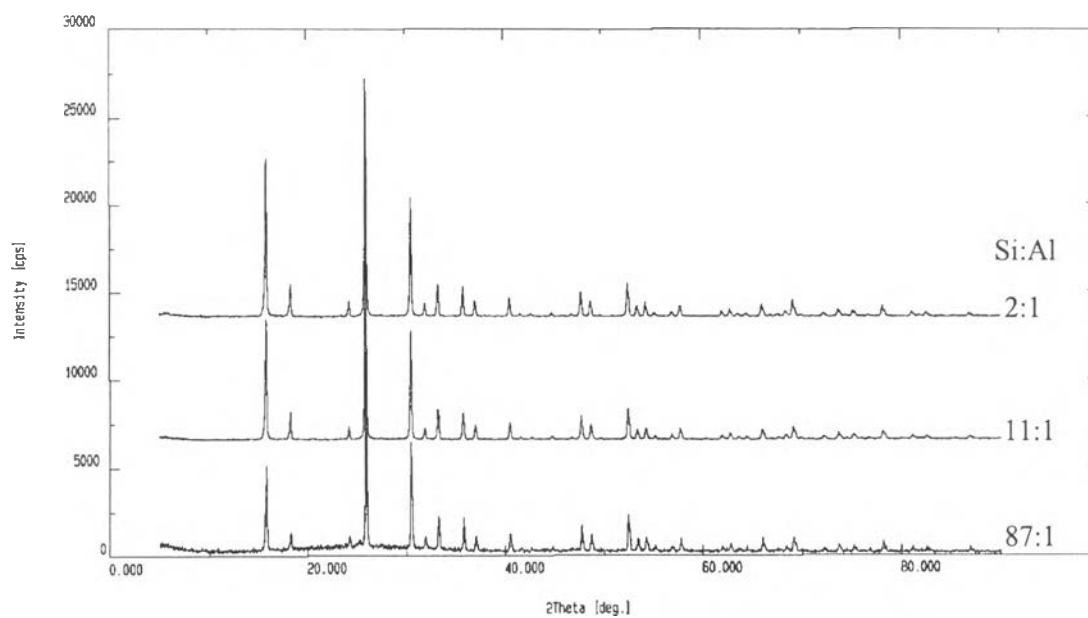


Figure 2.5 Effect of Si:Al ratio (2:1 – 87:1) on microwave heated aluminosilicate synthesized from $1\text{SiO}_2 \cdot x\text{Al}_2\text{O}_3 \cdot 3\text{Na}_2\text{O} \cdot 410\text{H}_2\text{O}$ ($x = 0.01149 - 0.25$) at $150^\circ\text{C}/15\text{h}$

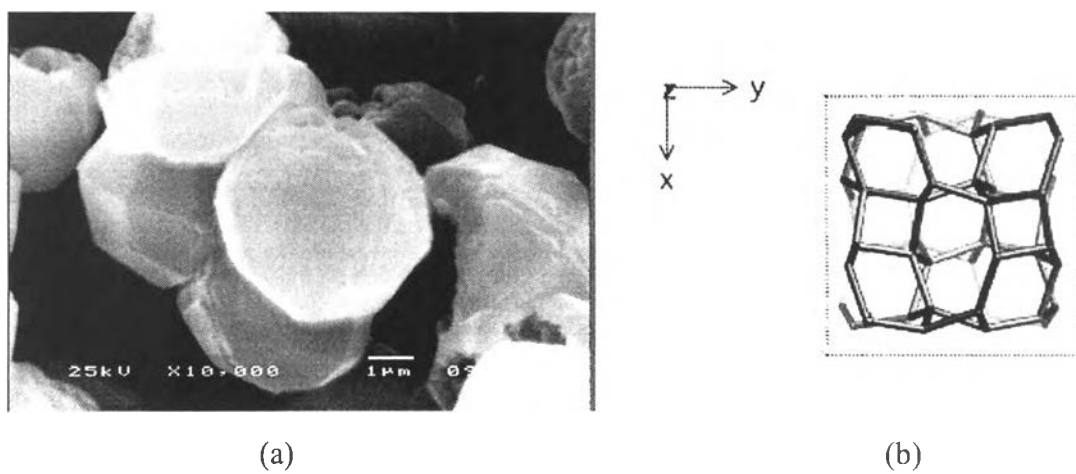


Figure 2.6 SEM micrographs of (a) Analcime zeolite (ANA) and (b) the unit cell structure

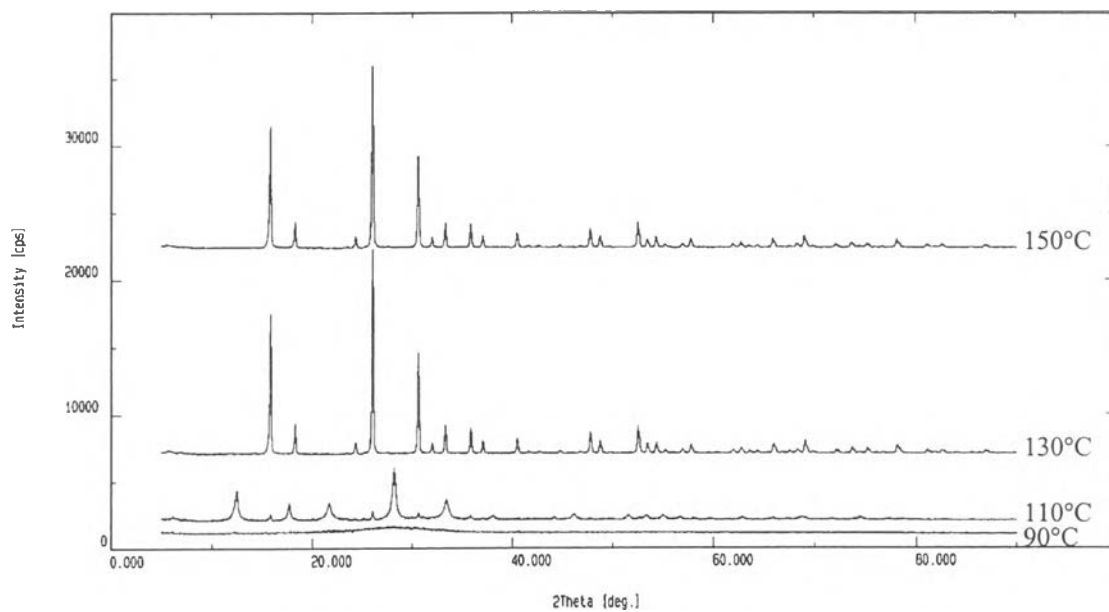


Figure 2.7 Effect of microwave heating temperature on aluminosilicate synthesized from $1\text{SiO}_2:0.091\text{Al}_2\text{O}_3:3\text{Na}_2\text{O}:410\text{H}_2\text{O}$ at $x^\circ\text{C}/15\text{h}$ ($x = 90^\circ - 150^\circ\text{C}$)

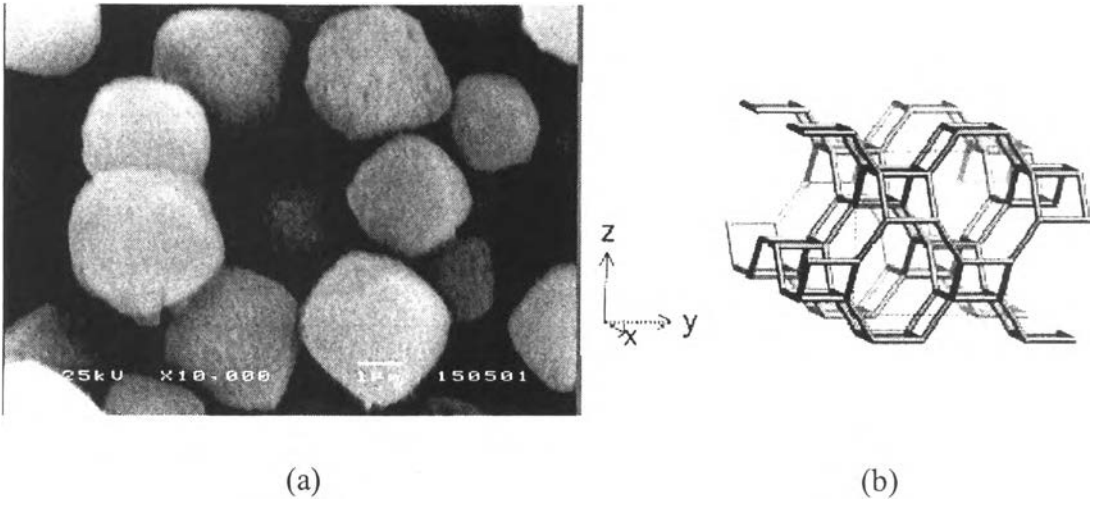


Figure 2.8 SEM micrographs of (a) Na-P1 zeolite (GIS) and (b) the unit cell structure

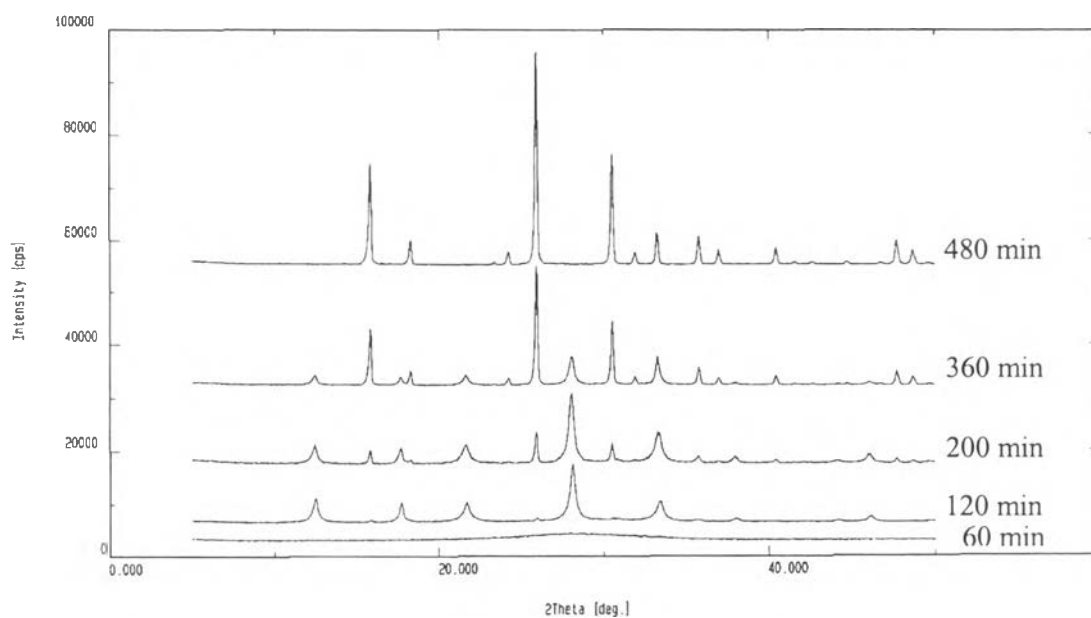


Figure 2.9 Effect of microwave heating time on aluminosilicate synthesized from $1\text{SiO}_2:0.25\text{Al}_2\text{O}_3:3\text{Na}_2\text{O}:410\text{H}_2\text{O}$ at $130^\circ\text{C}/x \text{ h}$ ($x = 1 - 9\text{h}$)

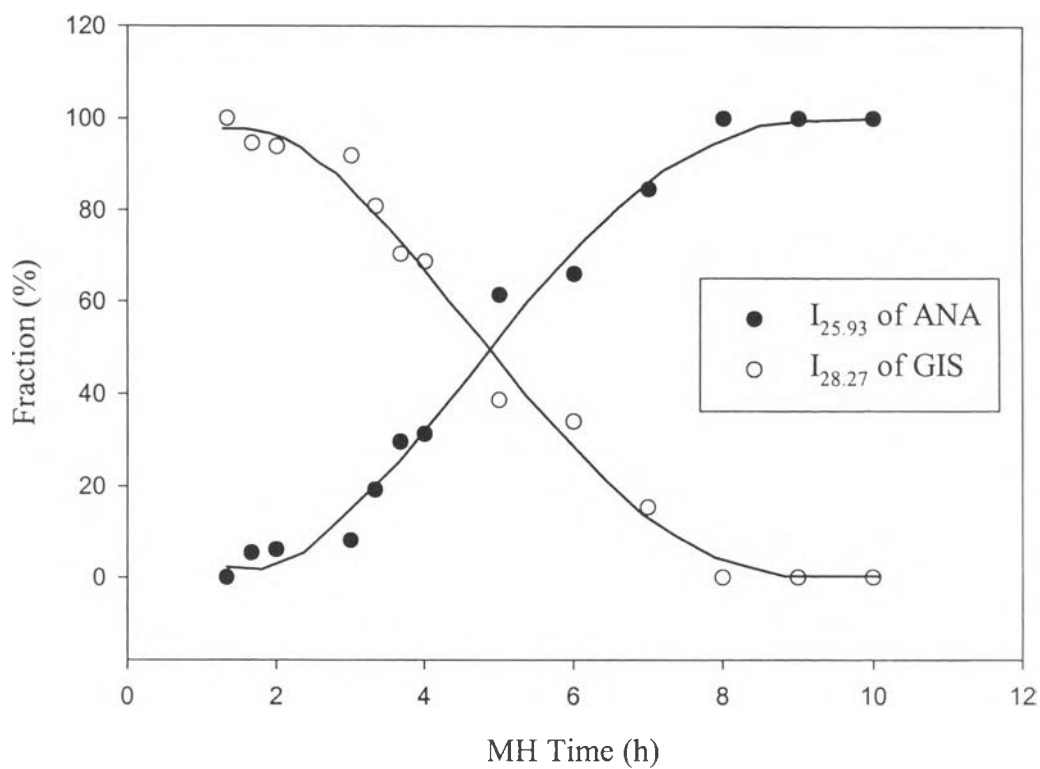


Figure 2.10 Fraction of GIS and ANA calculated from XRD area under the peak at 25.93 (2θ) for ANA and 28.27 (2θ) for GIS

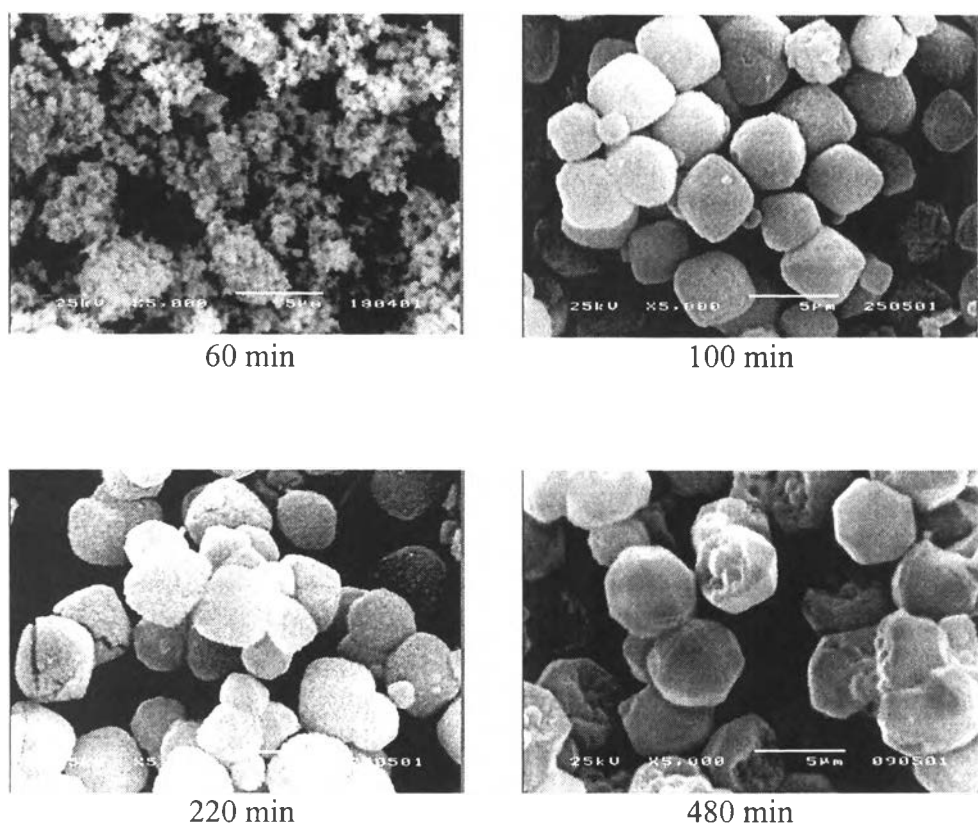


Figure 2.11 SEM micrographs of aluminosilicate synthesized from 1SiO_2 :
 $0.25\text{Al}_2\text{O}_3$: $3\text{Na}_2\text{O}$: $410\text{H}_2\text{O}$ at $130^\circ\text{C}/x\text{ h}$ ($x = 1 - 9\text{h}$)

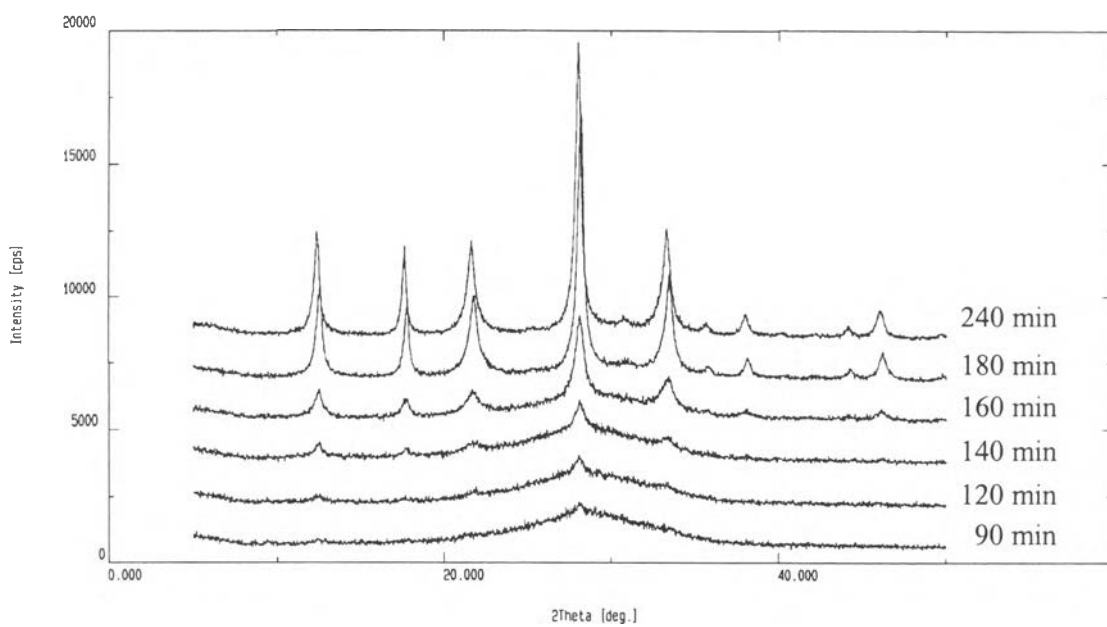


Figure 2.12 Effect of microwave heating time on aluminosilicate synthesized at $1\text{SiO}_2: 0.25\text{Al}_2\text{O}_3: 3\text{Na}_2\text{O}: 410\text{H}_2\text{O}$ and $110^\circ\text{C}/x \text{ h}$ ($x = 1.5 - 4\text{h}$)

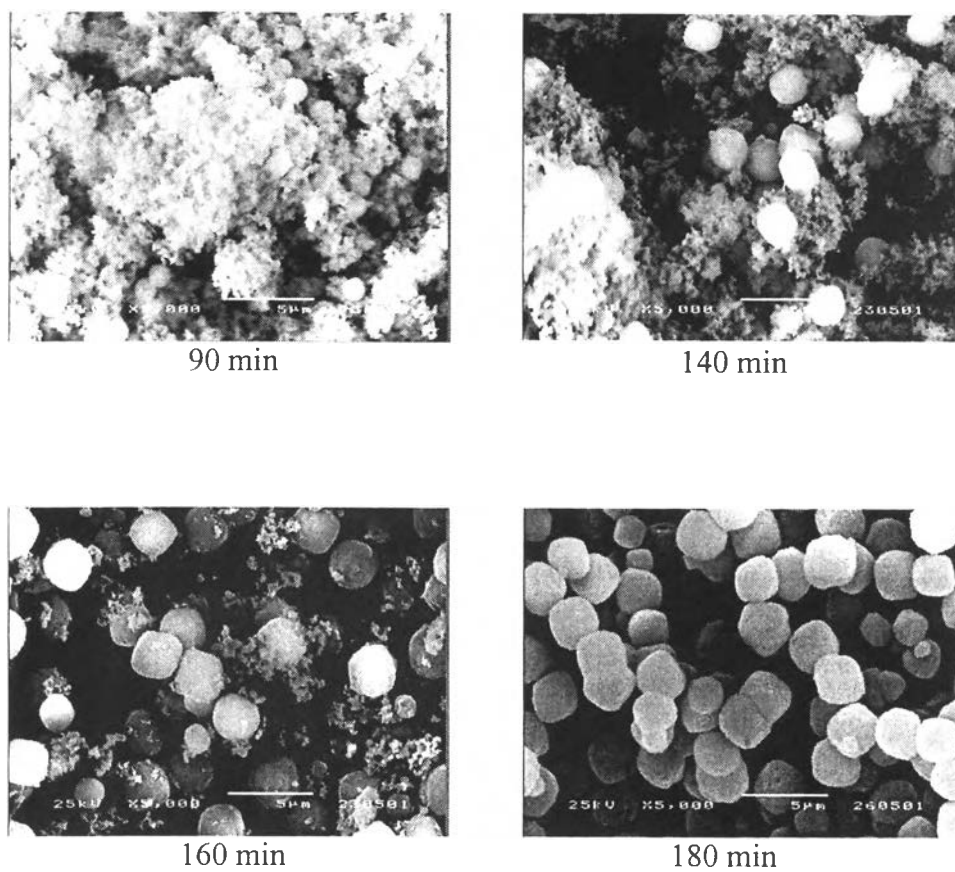


Figure 2.13 SEM micrographs of aluminosilicate synthesized from $1\text{SiO}_2:0.25\text{Al}_2\text{O}_3: 3\text{Na}_2\text{O}:410\text{H}_2\text{O}$ at $110^\circ\text{C}/x \text{ h}$ ($x = 1.5 - 4\text{h}$)